Original Article

Journal of Food Safety and Hygiene

Journal homepage: http://jfsh.tums.ac.ir

Iron-doped Biochar for effective removal of dissolved phosphate from the aqueous phase

Daryoush Sanaei[1*], Ali Salehi[2], Ebrahim Molaee-Aghaee[2], Nabi Shariatifar[2]

[1]*Department of Environmental Health Engineering, Faculty of Public Health and Safety, Shahid Beheshti University of Medical Sciences, Tehran, Iran.*

[2]*Division of Food Safety & Hygiene, Department of Environmental Health Engineering, School of Public Health, Tehran University of Medica Sciences, Tehran, Iran.*

ARTICLE INFO

Article history:
Received 12 Apr. 2021
Received in revised form
14 Jun. 2021
Accepted 25 Jun. 2021

Keywords:
Phosphorous adsorption;
Coconut fiber coir-based biochar;
Clean water;
Water quality

ABSTRACT

Due to the discharge of the effluent containing rich-nutrient matters such as phosphate into water bodies, some of the problems including eutrophication created that created adverse environmental impacts. Hence, we prepared a new Fe-doped coconut fiber coir-based biochar (Fe-CFCB) as an effective adsorbent for adsorbing phosphate from an aqueous solution. According to characteristics results, the amorphous structure besides the presence of ferrihydrite and hydroxide confirmed in the Fe-CFCB, enhances the phosphate adsorption. The pH and Temperature are played the main roles in phosphate adsorption by Fe-CFCB, according to batch experimental. the experimental data and before/after adsorption characteristics appeared that the electrostatic attraction, chemical precipitation, and complexation could be considered as main mechanisms of adsorption P by Fe-CFCB. The newly prepared adsorbent could reveal a feasible pathway for phosphate removal from an aqueous solution and also could consider an effective and eco-friendly adsorbent for the removal of wide ranges of pollutants in the future.

Citation: Sanaei D, Salehi A, Molaee-Ag haee E, Shariatifar N**. Iron-doped Biochar for effective removal of dissolved phosphate from the aqueous phase.** J food safe & hyg 2021; 7(2): 97-109.

1. Introduction

Until now, water polluted with various types of pollutants has been considered as a remarkable threat as it causes acute/chronic health risks to all ecosystems (1).

Phosphorus is an crucial nutrient element for all organisms and is essential for the functioning of ecosystems (2,3). The dissociation of phosphoric acid in aqueous phase occurred at pK_a 2.15, 7.20, and 12.35 for producing of $H_2PO_4^-$, HPO_4^{2-}, and PO_4^{3-} (4,5).

*Corresponding author. Tel.: +989384009473
E-mail address: daryoushsanaei@gmail.com.

The releasing of excess P into to aqueous solution causes eutrophication that further leads to the creating more problems such as generation of toxic algal blooms, and loss of biodiversity in water body (6,7). Thus, the removal of phosphate from water bodies by using promising techniques is of great importance.

Most of the research done to date on phosphate removal from water bodies, including electro-dialysis (8), electrocoagulation (9), reverse osmosis (10), adsorption (11,12), biological process (13,14), and chemical precipitation (15,16). Among the methods, adsorption process is considered as promising techniques to remove phosphate due to simple operation, cost-benefits, and design flexibility. The presence of different adsorbents, including carbon-based materials (e.g., biochar and carbon aerogel) (17-19), metal-based adsorbents (e.g., zero valent iron, Fe–Cu binary oxides, Fe–Zr binary oxide) (12,20,21), zeolites (22-24), synthetic polymers (e.g., polyvinyl alcohol) (25,26), and biomass-wastes (e.g., rice husk) (27,28) have been carried out for phosphate removal from water. However, the presence of main drawbacks from low adsorption capacity and weak chemical and mechanical stability to high cost and difficult handling, impeding their feasible application for remove of phosphate from aqueous bodies. Here, until recently, most of the researches still caried out to find out the reliable, cost-benefit, and sustainable materials to adsorb phosphate from water bodies and further achieving to enhance recovery P for improving food production (29).

Biochar is the most common material to remove various type of organic and inorganic contaminants as an adsorbent that is achieved by pyrolysis process of various biomass. The type of feedstock and thermo-synthesis properties are considered as main parameters that can significantly impact on adsorption capacity (30,31). Interestingly, most adsorbent, especially biochar matters suffer from week adsorption performance for anionic pollutants like phosphate due to the presence of not-attractive forces between adsorbent surfaces and phosphate ions (32,33). Therefore, which is more important to increase in the capability of the phosphate adsorption, being desirably modified or functional to pristine biochar. coconut fiber coir-based biochar (CFCB) is considered as an excellent feedstock to produce biochar because of high specific area, rich functional groups, and could be used as a promising adsorbent for removing of phosphate of aqueous solution.

Hence, in this study, a promising adsorbent for phosphate removal from aqueous solution was synthesized from coconut fiber coir-based biochar (CFCB) by doping Fe nanoparticles (Fe- CFCB). The Fe-CFCB adsorbent was investigated in terms of the effects of temperature, pH, and retention time on the phosphate adsorption capacity. Also, the Scanning electron microscopy (SEM), Ferrier transmittance IR (FTIR), and BET measurements performed to characterize CFCB and Fe-CFCB and also determine mechanisms of phosphate.

2.Materials and methods

2.1. Materials

KH_2PO_4 used as precursors to provide the stock solutions of Phosphate. The iron (III) chloride hexahydrate ($FeCl_3 \cdot 6H_2O$, 97%), and potassium dihydrogen phosphate (KH_2PO_4, 99.5%) were provided from Merk company. The production of CFCB using pyrolysis process under the ultrahigh purity of nitrogen and carbon dioxide gases.

2.2. Preparation of CFCB and Fe-CFCB

Biochar (CFCB) was prepared from coconut fiber coil as precursor's material. Coconut Fibers was separated from the shell of coconuts, grounded and dried at 60°C for 24 h at oven. Then, dried powder pyrolyzed at 800 °C under CO_2 atmosphere by rising rate of 10°C min^{-1} GSL-1700X, MTI Corporation, USA). The Fe-CFCB prepared by immersion of CFCB in 0.5 M $FeCl_3$ solution at 80°C for 6 h. after that, the results mixture washed with DI water to achieve natural material and then was dried at 105°C for 12 h. the obtained sample was referred as Fe-CFCB. The 0.1 M HCl or NaOH was carried out to adjust solution pH to 7.0.

2.3. Characterization of CFCB and Fe-CFCB

The surface morphology and elemental composition of prepared samples were determined using FE-SEM and EDX analysis (FE-SEM; Quanta 250 FEG). The BET method was performed to determine pore volume and specific surface area (Tris-Star II 3020 analyzer) under N_2 adsorption-desorption. The functional groups of as-synthesized samples were investigated by determining the peaks in the FTIR analysis. X-ray diffraction (XRD) analysis was carried out for identification of crystallographic structures of samples using Cu ka radiation at 45 kV (XRD, STOE-STADV).

2.4. Adsorption experiments

To evaluate the effect of pH on the phosphate adsorption capacity, batch experiments were carried out. After adsorption process, the suspension was filtered through a 0.45 µm membrane filter and then obtained solution to determine phosphate concentration was measured using a UV-VIS spectrophotometer at the 890 nm (Thermo Scientific; model Nicolet iS10). All the experiments were performed at 25°C in triplicate.

2.5. Adsorption isotherm

The Langmuir model used to estimate the adsorption performance, the formation of monolayer of dyes molecules on the adsorbent surface and the maximum adsorption capacity (Q_m) homogeneous surface of magnetite metal oxides/CAg due to adsorption process that written the linear and nonlinear forms it's as follows(34):

$$1/q_e = 1/Q_m + 1/k_L\, Q_m.\, 1/C_e \quad (1)$$

$$q_e = \frac{Q_m K_L C_e}{1+K_L C_e} \quad (2)$$

To describe heterogeneous adsorption and the behavior of a multilayer adsorption on the magnetite metal oxides/CAg surface, Freundlich isotherm was researched that obtained from the equation follows (35):

Linear form

$\ln q_e = \ln k_F + 1/n \ln C_e$ (3)

Non-linear form

$$q_e = k_F C_e^{\frac{1}{n}} \quad (4)$$

K_F is The Freundlich adsorption capacity and n is represented of adsorption heterogeneity.

2.6. Adsorption kinetics

The linear and Non-linear equations of pseudo- first order, pseudo- second-order, and Elovich were determined as follows (11, 36):

Linear form

$\ln (q_e - q_t) = \ln (q_e) - k_1.t$ (5)

$$\frac{t}{q_t} = \frac{1}{q_{e^2}\, k_2} + \frac{1}{q_e} t \quad (6)$$

$$q_t = \frac{1}{\beta} \ln(\alpha\beta) + \frac{1}{\beta} lnt \quad (7)$$

Non-linear form

$$\frac{dq_t}{dt} = k_1(q_e - q_t) \quad (8)$$

$$\frac{dq_t}{dt} = k_2(q_e - q_t)^2 \quad (9)$$

$$\frac{dq_t}{dt} = \alpha e^{-\beta_{qt}} \quad (10)$$

Where k_1, k_2, and α are the constant of pseudo-first, pseudo-second, and Elovich models, respectively. The β parameter is linked to the expanded coverage of surface and also activation energy for chemical adsorption (g mg^{-1}).

3.Results

3.1. Characterization of the CFCB and Fe-CFCB

The elemental composition of as-prepared samples is brought out in Table 1. The Fe content in the Fe-CFCB significantly increased in comparison of CFCB, while the other elemental content such as Al, Ca, and Mg decreased. As shown in Fig.1(a) and (b), The Fe-CFCB contained mainly metallic element distributions than that of CFCB.

The CFCB and Fe-CFCB appeared relatively higher specific surface area by measuring N_2 adsorption-desorption that were 745 and 521 m^2 g^{-1}, respectively (Fig. 2b, 2c and Table 2). The FTIR spectra of Fe-CFCB before and after adsorption process were depicted in Fig.3.

3.2.Adsorption isotherms

The experimental data were fitted by Langmuir, and Freundlich isotherms (Fig.4), and the ascribing parameters were reported in Table 3.

3.3. Sorption kinetics

Three kinetic profiles of adsorption by the CFCB and Fe-CFCB are depicted in Fig.5 and the obtained parameters were provided in Table 4.

3.4. Effects of pH

One of the most critical parameters affecting the adsorption process is pH value. As shown in Fig. 6, the adsorption of phosphate by CFCB and Fe-CFCB was highly pH-dependent.

Table 1. Chemical composition of CFCB and Fe-CFCB

Samples	Fe (mg g^{-1})	Ca (mg g^{-1})	Mg (mg g^{-1})	Al (mg g^{-1})	C (%)	N (%)	H (%)	O (%)	O/C
CFCB	1.61	5.1	2.65	2.36	84.31	0.48	1.54	13.54	0.16
Fe-CFCB	106.6	3.44	0.86	0.78	28.89	0.42	5.28	32.18	1.11

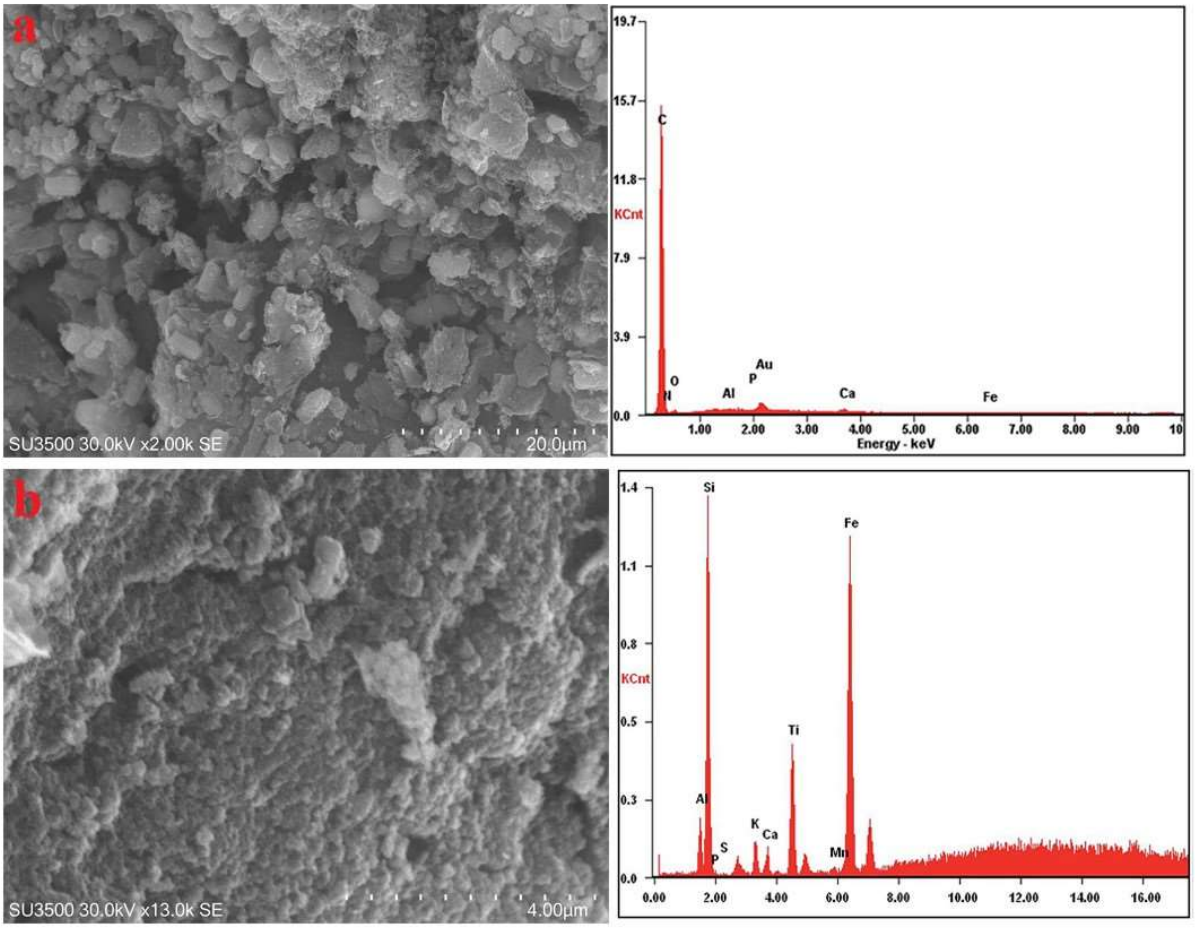

Figure1. FE-SEM and EDX images of the CFCB (a) and Fe-CFCB (b).

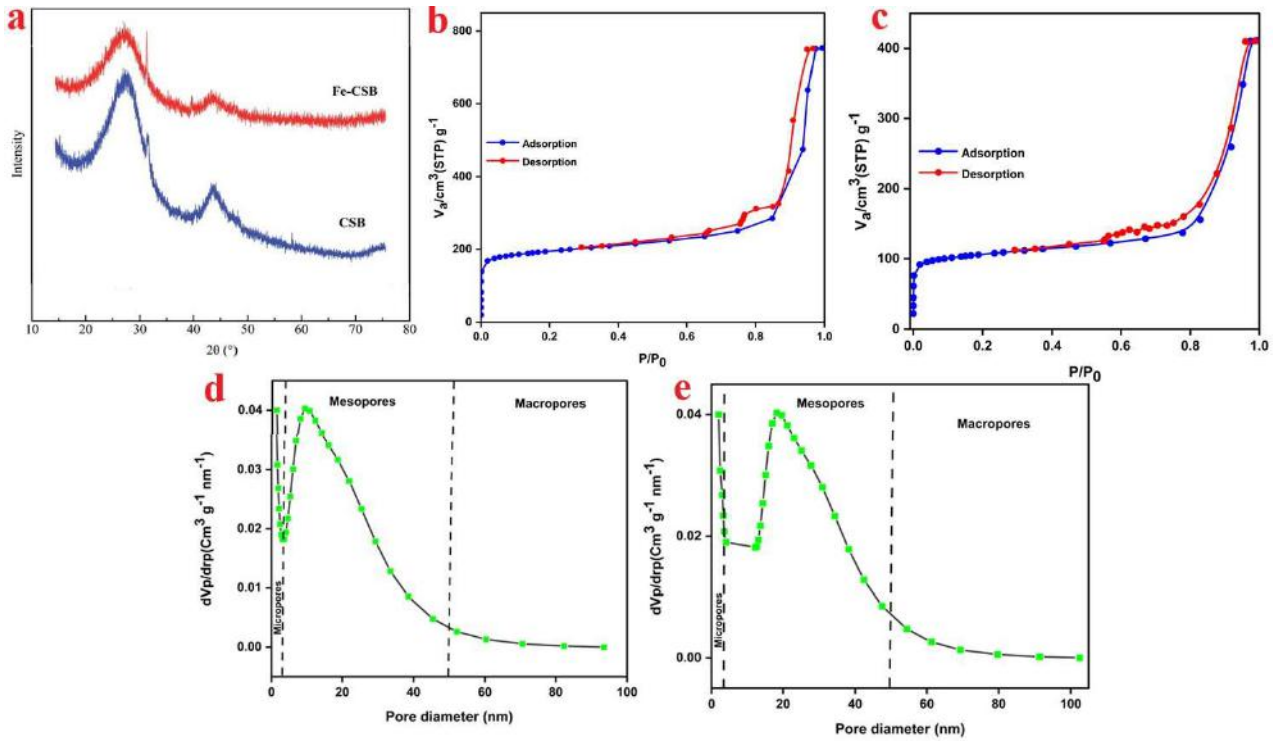

Figure.2 (a) XRD spectra of as prepared samples; Adsorption-desorption isotherms of (b) CFCB and (c) Fe-CFCB; and pore size distribution of (d) CFCB and (e) Fe-CFCB

Table 2. Physicochemical characteristics of CFCB and Fe-CFCB

Items	CFCB	Fe-CFCB
pH	6.7	7.9
BET ($m^2 g^{-1}$)	745	521
Surface area of micropore ($m^2 g^{-1}$)	584	334
Surface area of mesopore ($m^2 g^{-1}$)	161	187
Average pore diameter (nm)	2.3	2.8
Total pore volume ($cm^3 g^{-1}$)	0.44	0.36

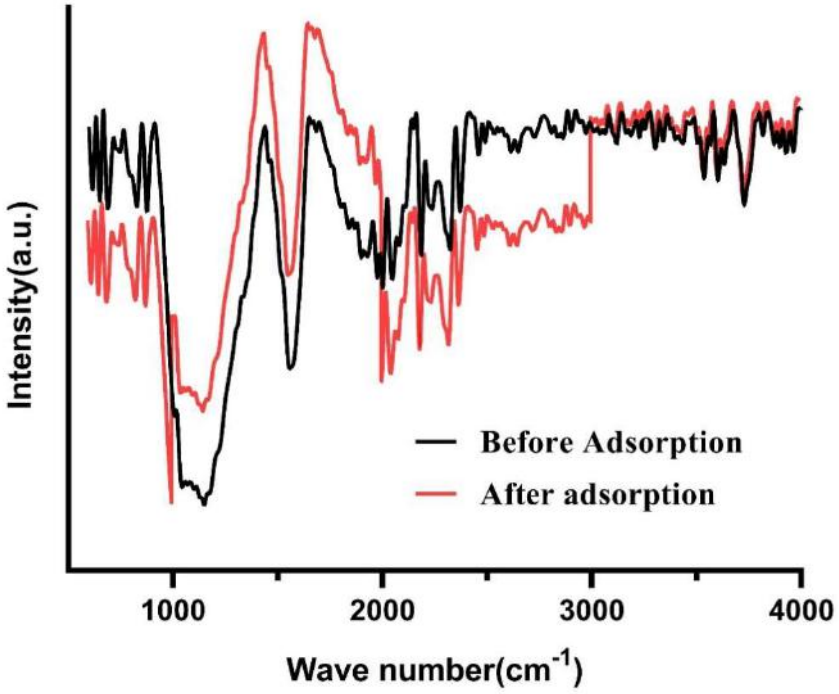

Figure3. FTIR spectra of Fe-CFCB before /after adsorption.

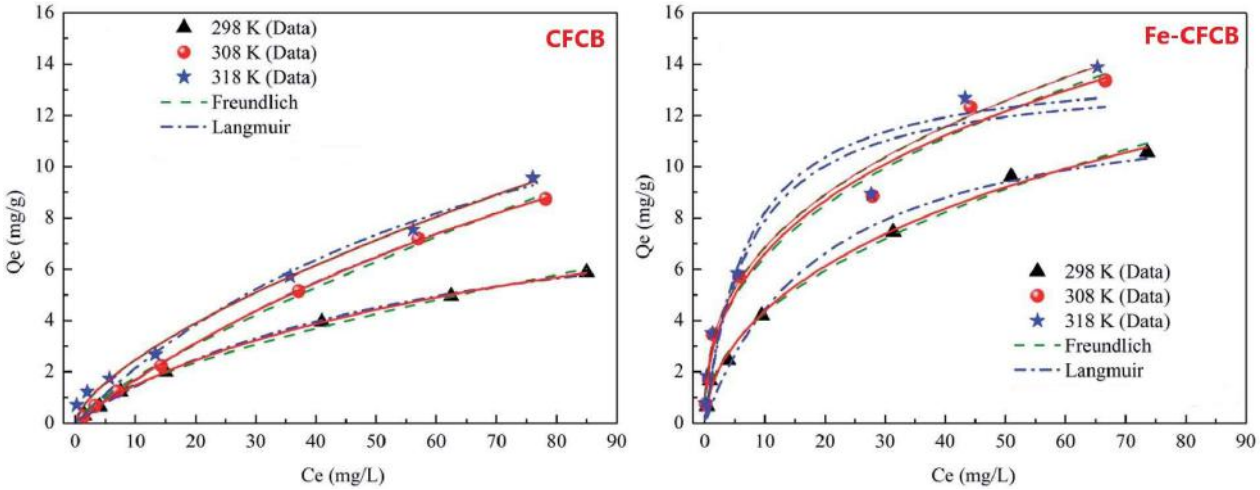

Figure 4. Adsorption isotherms and modeling of as-prepared samples at different temperatures.

Table 3. Isotherm parameters for adsorption of phosphate by CFCB and Fe-CFCB

parameters	CFCB			Fe-CFCB		
Langmuir	298 K	308 K	318 K	298 K	308 K	318 K
Q_m[a]	10.25	17.22	21.23	15.01	27.56	37.23
K_L[b]	0.018	0.005	0.017	0.057	0.141	0.148
R^2	0.998	0.996	0.98	0.974	0.954	0.923
RMSE[c]	0.075	0.067	0.47	0.62	1.052	1.322
Freundlich						
K_F[d]	0.017	0.004	0.011	0.038	0.045	0.0421
n[e]	0.884	0.952	0.912	0.572	0.441	0.435
R^2	0.99	0.999	0.995	0.995	0.982	0.987
RSME	0.037	0.057	0.256	0.311	0.595	0.60

[a] maximum adsorption capacity
[b] Langmuir constant
[c] error analysis
[d] Freundlich constant
[e] heterogenicity of adsorbent surface

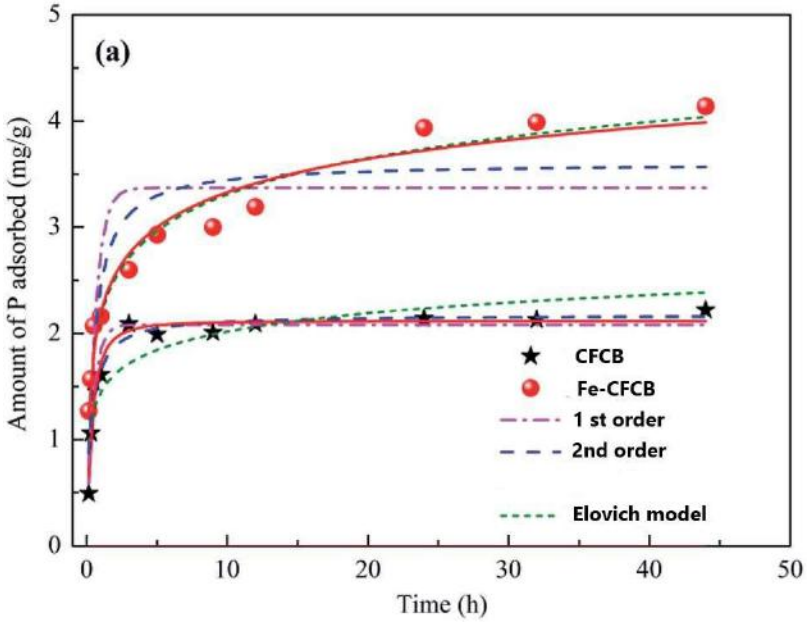

Figure 5. Kinetic modeling for P adsorption onto CFCB and Fe-CFCB.

Table 4. Kinetic parameters of adsorption P by as-prepared samples

Adsorbent	Model	Parameters	R^2	RMSE
CFCB	1st order	K_1=2.242	0.951	0.109
	2nd order	K_2 =1.512	0.961	0.106
	Elovich	b =4.011	0.892	0.228
Fe-CFCB	1st order	K_1=1.787	0.875	0.512
	2nd order	K_2 =0.623	0.863	0.395
	Elovich	b =2.021	0.977	0.247

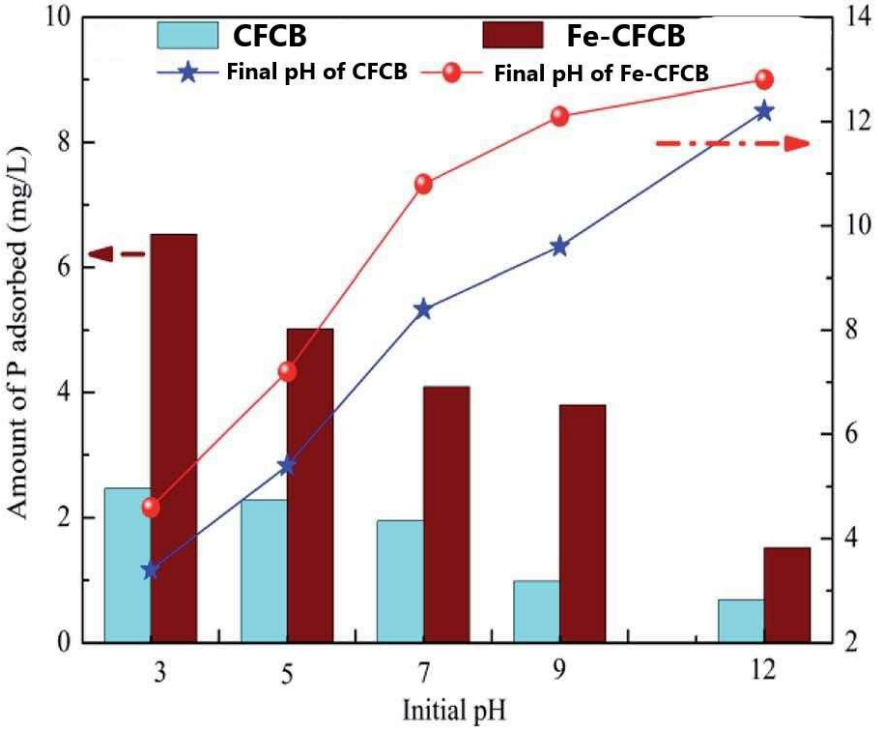

Figure 6. The initial pH influenced by adsorption of phosphate on the as-prepared adsorbents

4.Discussion

The XRD spectra exhibited that the CFCB was contained mainly cellulose crystal plane that found out at a broad peak of 23.0° (**Fig.2a**). by doping Fe nanoparticles into CFCB, beside diffraction peaks of 26 °, 43.5°, and 44.1° that ascribed to caron, three new peaks revealed that are located at 30.5°, 36°, and 57.7°, matching well with Fe_3O_4 and Fe_2O_3 structures (**Fig.2a**). Because of incorporation of Fe nanoparticles into micro-mesoporous structures of CFCB, some of porous channels of CFCB are blocked and thereby reduced partially BET surface area. Interestingly, the CFCB and Fe-CFCB have zeta potentials of -39.2 mV and 24.4 mV, respectively.

The content of the iron hydroxide and oxygen-containing groups on the surface of Fe-CFCB caused a changing in the zeta potential. The Fig. 2d, and Fig. 2e showed the pore size of CFCB and Fe-CFCB, indicating a partial increasing of pore diameter from 2.7 nm for CFCB to 3.2 nm for Fe-CFCB.

The observing of three new peaks at 625, 535, and 451 cm^{-1} in Fe-CFCB after phosphate adsorption that was corresponding to the Fe-O/Fe-N stretching, confirming the main roles of the Fe-O or Fe-N bonds in phosphate adsorption(37). Moreover, the vibration peaks of 960, 1055, and 1150 cm^{-1} in Fe-CFCB after adsorption of P, ascribing to the P-O bonds and firmly adsorbed on the surface of the Fe-CFCB.

It is clearly seen that the obtained data from adsorption P by adsorbents were fitted well with Freundlich model due to estimated higher R^2 and lower RMSE values. These results indicates that the phosphate adsorption of behavior by CFCB and Fe-CFCB could more precisely explained by Freundlich model. This observation concluded that the heterogenicity of surface and multilayer adsorbed phosphate could be considered as dominant mechanisms of adsorption. The maximum adsorption capacity (Q_{max}) for Fe-CFCB calculated from model was about 65.32 mg g^{-1}.

The lower RMSE and higher R^2 values showed a better fitting of the experimental data with Elovich model. It is concluded that the adsorption of P onto Fe-CFCB might be controlled by more sorption mechanisms (38-40).

For CFCB, the adsorption capacity decreased further by increasing of pH from 3 to 12. While the adsorption capacity partially decreased by increasing of pH from 3 to 12 than that of CFCB. The monovalent $H_2PO_4^-$ and divalent HPO_4^{2-} were dominant species in the pH ranges of 3-7 and 7-9, respectively. The pH_{zpc} of Fe-CFCB was 7.6 that protonated at low pH. In turn, the positive charge of surface Fe-CFCB might be adsorbed the negatively charged P anions. the strong attraction at lower pH is considered as main reason in the higher adsorption capacity of Fe-CFCB. While the higher pH caused the more negative charges maintained on the surface of Fe-CFCB and CFCB, generating a strong repulsive between main phosphate species and surface of CFCB and Fe-CFCB.

5.Conclusion

In this work, Fe-doped coconut fiber coir-based biochar (Fe-CFCB) were successfully prepared and investigated for phosphate removal from aqueous solution. The clear distinguish of CFCB by doping Fe are observed by performing FE-SEM, EDX, and BET analysis. Fe-CFCB revealed a greater phosphate adsorption capacity than that of CFCB. The maximum phosphate adsorption capacity (Q_{max}) of Fe-CFCB was 65.32 mg P g^{-1},

confirming that Fe-CFCB had enhanced phosphate removal, compared to pure CFCB. The experimental data were fitted well by Freundlich model and Elovich kinetic. The adsorption capacity of Fe-CFCB was remarkably influenced by the pH and decreased as pH increased from 3 to 12. It was demonstrated that the adsorption process is an exothermic process, and the phosphate adsorption increased as the temperature increased. This could be related to increase activity of adsorbent sites on the Fe-CFCB. it is important to note that the Phosphate adsorption on Fe-CFCB is also influenced by time that revealed is the fast at first 4 h and then reached levelly until the plateau of adsorption was achieved.

The results demonstrated that Fe-CFCB could have a great potential of being eco-environmental adsorbent for phosphate removal and possible potential for other organic and/or inorganic in the future from aqueous solution.

Conflict of interest

The authors confirm there is no conflict of interest.

Acknowledgments

This study is in support of the project NO 11906 assigned by the Student Research Committee, Shahid Beheshti University of Medical Sciences, and Department of Environmental Health Engineering, School of Public Health, Tehran University of Medical Sciences, Tehran, Iran.

References

1. Dehghani MH, Sarmadi M, Alipour MR, et al, Investigating the equilibrium and adsorption kinetics for the removal of Ni (II) ions from aqueous solutions using adsorbents prepared from the modified waste newspapers: A low-cost and available adsorbent. Microchem J 2019; 146: 1043-53.
2. Alipour M, Massoudinejad M, Sanaei D, et al. Design and synthesis of two novel carbon aerogels using citric and tartaric acids as catalysts for continuous water desalination. desalin. Water Treat 2021; 215: 69-79.
3. Sarmadi M, Foroughi M, Saleh H, et al. Nefficient technologies for carwash wastewater treatment: a systematic review. Environ Sci Pollut Res Int 2020: 1-17.
4. Mahvi AH, Sarmadi M, Sanaei D, et al, Removal of lead ion from aqueous solutions by adsorption onto phosphate-functionalized treated waste papers (PF-TWPs). Desalination Water Treat 2020; 200: 205-216.
5. Dehghani MH, Sanaei D, Nabizadeh R, et al. Source apportionment of BTEX compounds in Tehran, Iran using UNMIX receptor model. Air Qual Atmos Health 2017; 10: 225-234.
6. Salehi A, Khaniki GJ, Shoghi K ,et al. Microbial evaluation of cooked foods served in the central restaurant of Tehran university of medical sciences in winter and summer 2015. Iranian Health, Safety & Envir 2016; 3: 621-25.
7. Dehghani MH, Sanaei D, Ali I, et al. Removal of chromium (VI) from aqueous solution using treated waste newspaper as a low-cost adsorbent: kinetic modeling and isotherm studies. J Mol Liq 2016; 215: 671-79.

8. Yang Yu, Jenyuk L, Satoshi T. Hybrid ferrihydrite-MF/UF membrane filtration for the simultaneous removal of dissolved organic matter and phosphate. Water Res 2014; 65: 177-185.
9. Zhang X, Lin H, Wei W, et al. Electrocoagulation of dairy manure using low-carbon steel electrodes for phosphorus removal. J Environ Eng 2020; 146: 04020044.
10. Javier L, Farhat NM, Vrouwenvelder JS. Enhanced hydraulic cleanability of biofilms developed under a low phosphorus concentration in reverse osmosis membrane systems. Water res X 2021; 10: 100085.
11. Li S, Lei T, Jiang F, et al. Tuning the morphology and adsorption capacity of Al-MIL-101 analogues with Fe3+ for phosphorus removal from water. J Colloid Interface Sci 2020; 560: 321-29.
12. Zhang L, Dan H, Bukasa OT, et al. Low-cost efficient magnetic adsorbent for phosphorus removal from water. ACS omega 2020; 5: 25326-25333.
13. Roots P, Sabba F, Rosenthal AF, et al. Integrated shortcut nitrogen and biological phosphorus removal from mainstream wastewater: Process operation and modeling. Environmental: Water & Tech 2020; 6: 566-80.
14. Xu Q, Liu X, Yang G, et al. Norfloxacin-induced effect on enhanced biological phosphorus removal from wastewater after long-term exposure. J Hazard Mater 2020; 392: 122336.
15. Bertanza G, Menoni L, Capoferri GU, et al. Promoting biological phosphorus removal in a full scale pre-denitrification wastewater treatment plant. J Environ Manage 2020; 254: 109803.
16. Park Y, Gorman C, and Ford E. Lanthanum carbonate nanofibers for phosphorus removal from water. J Mater Sci 2020; 55: 5008-20.
17. Jiao GJ, Ma J, Li Y, et al. Enhanced adsorption activity for phosphate removal by functional lignin-derived carbon-based adsorbent: Optimization, performance and evaluation. Sci Total Environ 2021; 761: 143217.
18. Ajiboye TO, Oyewo OA, Onwudiwe DC, et al. Adsorption and photocatalytic removal of rhodamine b from wastewater using carbon-based materials. Flat Chem 2021; 29: 100277.
19. Lebrun M, Van Poucke R, Miard F, et al. Effects of carbon-based materials and redmuds on metal (loid) immobilization and growth of salix dasyclados Wimm. on a former mine technosol contaminated by arsenic and lead. Land Degrad & Develop 2021; 32: 467-81.
20. Yang Z, Zhu T, Xiong M, et al. Tuning adsorption capacity of metal–organic frameworks with Al3+ for phosphorus removal: Kinetics, isotherm and regeneration. Inorg Chem Commun 2021; 132: 108804.
21. Devi P, Saroha AK. Methods used for performance enhancement of iron-based magnetic adsorbents in water systems. advanced magnetic adsorbents for water treatment. Springer, Cham 2021; 467-92.
22. Lin H, Ma R, Lin J, et al. Positive effects of zeolite powder on aerobic granulation: nitrogen and phosphorus removal and insights into the interaction mechanisms. Environ Res 2020; 191: 110098.
23. Feng J, Jiang L, Yuan B, et al. Enhanced removal of aqueous phosphorus by Zr,Fe, Mn–Fe-, and Mn–Zr–Fe-modified natural zeolites: comparison studies and adsorption mechanism. Environ Eng Sci 2020; 37: 572-84.
24. Dong Y, Lin H, Zhang X. Simultaneous ammonia nitrogen and phosphorus removal from micro-polluted water by biological aerated filters with

different media. Water Air Soil Pollut 2020; 231:1-15.

25. Peng Z, Jiang K, Lou T, et al. Enhanced denitrification of secondary effluent using composite solid carbon source based on agricultural wastes and synthetic polymers. Water Sci Technol 2021; 83: 886-93.
26. Zhao J, Yuan Q, Sun Y. Effect of fluoxetine on enhanced biological phosphorus removal using a sequencing batch reactor. Bioresour Technol 2021; 320: 124396.
27. Vaish B, Srivastava V, Singh PK, et al. Energy and nutrient recovery from agro-wastes: rethinking their potential possibilities. Environ Eng Res 2020.
28. Bargougui L, Chaieb M, Mekki A. Monitoring cocomposting of Agro-Wastes from olive mill by-products and poultry manures. Environ Eng Sci 2020. 37: 728-36.
29. Muisa N, Nhapi I, Ruziwa W, et al. Utilization of alum sludge as adsorbent for phosphorus removal in municipal wastewater: a review. J Water Process Eng 2020. 35: 101187.
30. Mclennon E, Solomon Jk, Neupane D, et al. Biochar and nitrogen application rates effect on phosphorus removal from a mixed grass sward irrigated with reclaimed wastewater. Sci Total Environ 2020; 715: 137012.
31. Qian T, Lu D, Soh YNA. Biotransformation of phosphorus in enhanced biological phosphorus removal sludge biochar. Water Res 2020; 169: 115255.
32. Yuan J, Wen Y, Ruiz G, et al. Enhanced phosphorus removal and recovery by metallic nanoparticles-modified biochar. Nanotech Environ Engin 2020; 5: 1-13.
33. Arun J, Gopinath KP, Vigneshwar S, et al. Sustainable and eco-friendly approach for phosphorus recovery from wastewater by hydrothermally carbonized microalgae: study on spent bio-char as fertilizer. J Water Process Eng 2020; 38: 101567.
34. Wu F, Yu Q, Gauvin F. Phosphorus removal from aqueous solutions by adsorptive concrete aggregates. J Cleaner Prod 2021; 278: 123933.
35. Su JF, Li GQ, Wen Q, et al. Highly efficient nitrate and phosphorus removal and adsorption of tetracycline by precipitation in a chitosan/polyvinyl alcohol immobilized bioreactor. Bioprocess. Biosyst Eng 2020 43; 10: 1761-71.
36. Zhang B, Zhao Z, Chen N, et al. Insight into efficient phosphorus removal/recovery from enhanced methane production of waste activated sludge with Chitosan-Fe supplementation. Water Res 2020; 187: 116427.
37. Guerra AAAM, Campos AFC, de Lima RM, et al. Efficient uptake of phosphorus from water by core@ shell bimagnetic nanoadsorbents. J Environ Chem Eng 2020; 8: 103888.
38. Jia Z, Zeng W, Xu H, et al. Adsorption removal and reuse of phosphate from wastewater using a novel adsorbent of lanthanum-modified platanus biochar. Process Safety and Enviro Protec 2020; 140: 221-32.
39. Lei Y, Geraets E, Saakes M, et al. Electrochemical removal of phosphate in the presence of calcium at low current density: Precipitation or adsorption? Water Res 2020; 169: 115207.
40. Eljamal O, Thompson IP, Maamoun I, et al. Investigating the design parameters for a permeable reactive barrier consisting of nanoscale zero-valent iron and bimetallic iron/copper for phosphate removal. J Mol Liq 2020; 299: 112144.